Direct measurement of drug–enzyme interactions by atomic force microscopy; dihydrofolate reductase and methotrexate

Shellie M. Rigby-Singleton, Stephanie Allen, Martyn C. Davies, Clive J. Roberts, Saul J. B. Tendler * and Philip M. Williams

Laboratory of Biophysics and Surface Analysis, School of Pharmaceutical Sciences, The University of Nottingham, University Park, Nottingham, UK NG7 2RD. E-mail: Saul.Tendler@nottingham.ac.uk; Fax: 0115 9515110; Tel: 0115 9515046

Received (in Cambridge, UK) 3rd May 2002, Accepted 12th July 2002
First published as an Advance Article on the web 23rd August 2002

There is a wealth of structural information on the drug–enzyme complex, dihydrofolate reductase and methotrexate. However, the dissociation dynamics of the complex remain relatively poorly understood. This paper describes the application of the atomic force microscope to quantify the rupture forces upon the forced dissociation of the ligand from the enzyme. The intermolecular forces experienced between dihydrofolate reductase and methotrexate as a binary and ternary complex, and the effect of pH upon these forces were studied. The rate at which forced dissociation occurs is known to have a significant effect upon the forces experienced between receptor–ligand complexes. This dependency of rupture force upon retract velocity is investigated. A linear relationship between force and the logarithm of velocity is demonstrated for the forced dissociation of the binary complex, inferring the presence of a barrier in the energy landscape positioned approximately 3 Å away from the bound state. The influence of the cofactor, NADPH, upon these rupture forces was negligible, suggesting that the barrier probed does not facilitate the cooperativity of the ternary complex. However, protonation of the Asp26 residue situated deep within the methotrexate binding site results in a decrease in rupture force.

Introduction

Dihydrofolate reductase (DHFR) is a biologically ubiquitous enzyme, which catalyses the NADPH-dependent reduction of 7,8-dihydrofolate to 5,6,7,8-tetrahydrofolate. Tetrahydrofolate serves as a coenzyme in numerous one-carbon transfer reactions, which are essential for the biosynthesis of purines and pyrimidines, including thymidylate, and several amino acids.[1] Due to the fundamental involvement of DHFR in biosynthesis, the enzyme has been exploited as a target for various therapies, including anticancer (methotrexate), antibacterials (trimethoprim), and antimalarials (pyrimethamine) for almost half a century.[1]

The 3-dimensional structures of various species of DHFR in its free,[2] binary [3–5] and ternary complexes [3–6] (Fig. 1a) [3] have been elucidated using NMR spectroscopy and X-ray crystallography. The extensive studies undertaken using X-ray crystallography have provided an insight into the different conformational states of the enzyme, throughout the progressive stages of complex formation.[5] A conformational dependence of the ternary complex (DHFR–folate–NADPH) on pH has also been demonstrated through NMR.[7,8]

High-resolution crystal structures of the enzyme–inhibitor complex have also been elucidated.[2,5,9–11] In particular, the inhibitor methotrexate (MTX) has been studied extensively over the last half century (Fig. 1b). Methotrexate upon binding to DHFR inhabits the same hydrophobic binding site as folate. Demonstrating a higher binding affinity for DHFR than folate, methotrexate acts as a competitive inhibitor of DHFR. When bound, methotrexate adopts an inverse orientation compared to that of folate, but retains the same hydrogen bonding geometry as the enzyme–substrate complex.[2] The binding site is configured of the αB helix (residues 24–32,*lc* (*Lactobacillus casei*)), a loop (49–57,*lc* which forms a part of the active site) connecting the αC helix (43–48,*lc*) to the βC sheet (58–62,*lc*), and a 9 to 23,*lc* residue loop (connecting the βA sheet and the αB helix).[2,3]

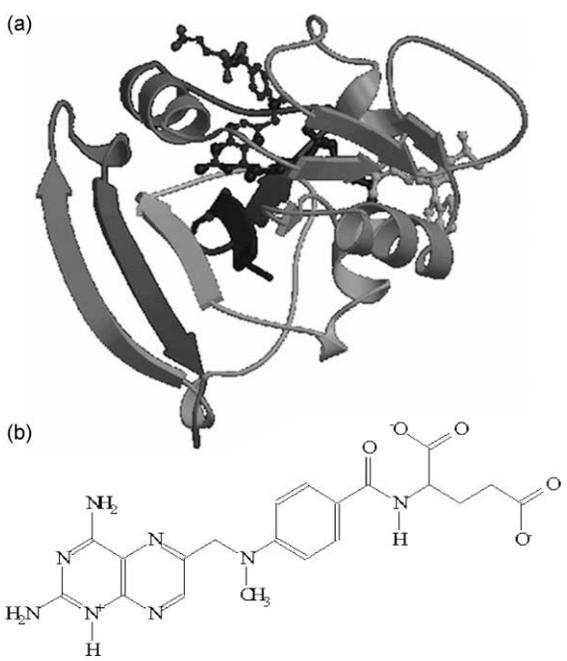

Fig. 1 (a) The crystal structure of *Lactobacillus casei* DHFR complexed with methotrexate and NADPH (Bolin *et al.*, 1982) [3]; (b) the chemical structure of methotrexate.

The 9 to 23 loop can exist in various conformations in different complexes, namely in an "open", "closed", "occluded" or "disordered" state with respect to the active site.[5] The solution structure of the DHFR–methotrexate complex determined by NMR indicates that the 9–23 loop is present in a closed conformation.[11] As a binary complex, a number of intermolecular bonds are formed directly and indirectly between methotrexate and DHFR (Table 1). The availability of such structural data

 DOI: 10.1039/b204290h

Table 1 Hydrogen bonds formed between *Lactobacillus casei* DHFR and methotrexate; ⟶ Hydrogen bond

Constituent of methotrexate	Bond formed with *Lactobacillus casei* DHFR		Ref.
	DHFR	Details	
Pyrimidine			
4-amino grp	Leu 4-carbonyl grp		
	Ala 97-carbonyl grp		3
2-amino grp	Asp 26 (Oδ1)	⟶ Thr 116	
	Wat-201 (water molecule)	⟶ Thr 116 (γ-hydroxy)	3
		⟶ Asp 26 (Oδ1)	
		⟶ Leu 114	3,11
N1	Asp 26 (Oδ2)		
Pyrazine			
N8	Wat-253	⟶ Asp 26 (Oδ2)	3
		⟶ Wat-217	
		⟶ Leu 23 (amide N)	
		⟶ NεTrp 21	
Glutamate			
α-carboxylate	Arg 57-guanidinium		3,6,11
γ-carboxylate	His 28-imidazole		

provides an insight into the number and type of bonds involved in the association and dissociation pathways of the complex.

NMR spectroscopic studies reveal that the conformation of the binary complex is comparable to that of the ternary complex.[11] Furthermore, a cooperative relationship between the coenzyme and substrate/inhibitor has been readily observed.[12–18] Investigations have demonstrated that the binding constant of the coenzyme is dependent upon the structure of the coenzyme and the substrate/inhibitor.[16–18] However, the structural source of cooperativity remains elusive.

Conformational changes in the DHFR molecule that correspond with changes in environmental pH have also been reported using NMR techniques.[7,8] This dependency of conformation on pH has been linked to the protonation of the Asp26 residue.[7,8] The carboxylate group of the DHFR Asp26 is the only group available which may become protonated, leading to a disruption in bond formation in the ternary complex.[7,8]

Here we employ the AFM to investigate the rupture forces of the drug–enzyme complex in their binary and ternary conformations. We show a dependency of force required to rupture the DHFR–methotrexate complex on the rate of dissociation. The association and dissociation processes exhibited by receptor–ligand complexes occur at a state of equilibrium where zero force is applied.[19] If detachment is forced prior to diffusive unbinding then the bond will demonstrate dynamic strength. Thus, the required force is dependent upon the timeframe of the dissociation event. Such events recorded over a wide range of loading rates can be used to provide detailed maps of the energy landscapes which contour the dissociation pathway.[19] Since dissociation rate is exponentiated under force, a wide range of loading rates are required to explore the whole dissociation pathway.

Previous studies on the complex describe the structural conformations, and the association and dissociation constants for such conformational states of the enzyme. However, the dissociation kinetics over the unbinding pathway for the complex remains poorly understood. Through the combination of dynamic force spectroscopy, molecular modelling and the structural data, it is possible to elucidate the energy landscape of the unbinding process, providing thermodynamic and dissociation rate details over the complete dissociation landscape. However, due to the wide range of loading required the application of AFM for dynamic force spectroscopy is restricted to a limited region of the force spectrum. Thus, here we limit ourselves to a narrow region of the landscape, investigating the effect the cooperative relationship between coenzyme and inhibitor has upon this region, as well as the effect of pH on the unbinding process.

Results and discussion

In studying the rupture forces between the binary and ternary complex, silicon nitride AFM probes were functionalised by the attachment of a methotrexate-modified agarose bead. Rupture forces were recorded between the probe and an *L. casei* DHFR monolayer covalently attached to a silicon substrate (Fig. 2).

A typical force *versus* distance curve for a measurement performed between DHFR and methotrexate in 100 mM sodium phosphate buffer, pH 7.4 at a retract velocity of 0.5 μm s^{-1}, is displayed in Fig. 3. The specificity of interaction is characterised

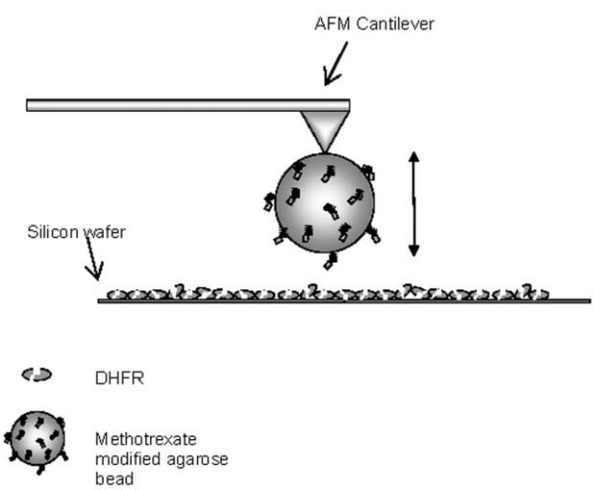

Fig. 2 Illustration of experimental procedure (not to scale).

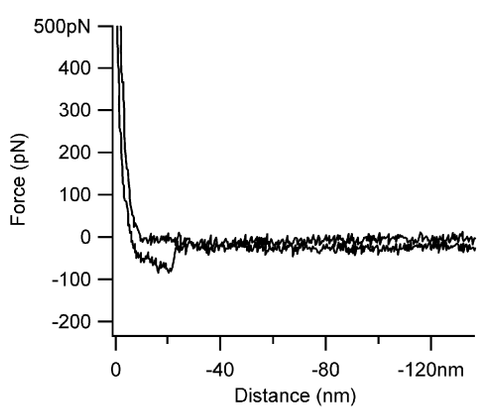

Fig. 3 A typical force curve between DHFR–methotrexate (0.5 μm s^{-1}, pH 7.4). *Fine black*, approach trace; *thick black*, retract trace.

by the non-linear stretch of the linker prior to detachment. In contrast, non-specific adhesion is illustrated by a continuation of the contact region upon retraction prior to a sharp pull off.[20]

Experimental retraction rates

Analysis of force measurements recorded for the DHFR–methotrexate complex over a range of retract rates produced a logarithmic relationship between rupture force and dissociation rate. A peak rupture force of 91 s.d. 25 pN was obtained for the unbinding of the binary complex at a retract velocity of 1.0 μm s^{-1} (Fig. 4a, *white histogram*). A decrease in force was

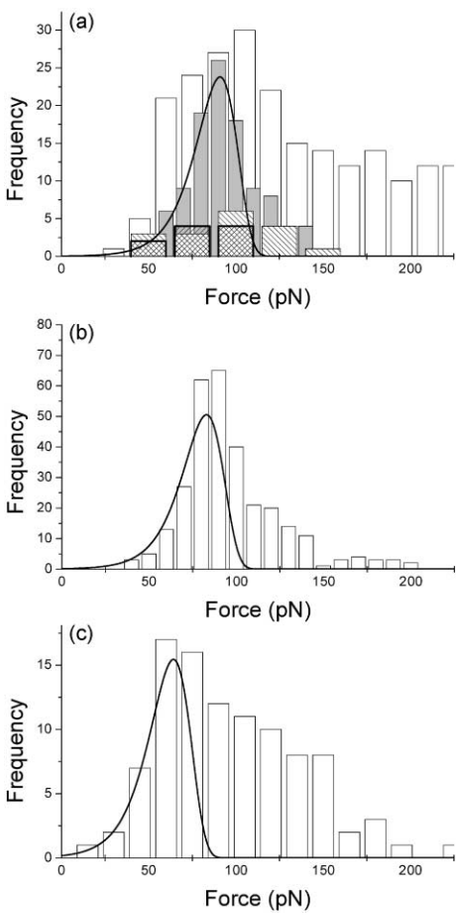

Fig. 4 Frequency distribution histograms for the binary complex performed in a 100 mM sodium phosphate, pH 7.4 environment at various retract velocities; (a) 1.0 μm s^{-1} yielding rupture forces of 91 s.d. 25 pN and 90 s.d. 16 pN (*white and grey* histograms, respectively), the *back slash* histogram represents the control block force measurements for the *white histogram* data, and the *forward slash* histogram for the control measurements for the *grey histogram* data; (b) 0.5 μm s^{-1} yielding rupture forces of 88 s.d. 16 pN; (c) 0.1 μm s^{-1} displaying rupture forces of 64 s.d. 14 pN. Superimposed upon the force histograms is a model distribution derived from the experimental force scale of 12 pN.

experienced with a decrease in velocity. At 0.5 μm s^{-1} a force of 88 s.d. 16 pN was required for rupture (Fig. 4b), and a further decrease in velocity to 0.1 μm s^{-1} led to a decrease in peak rupture force to 64 s.d. 14 pN, as depicted in Fig. 4c. Figs. 4a (*white histogram*) and 4c exhibit a wide distribution of rupture forces with long tails to high force, which are indicative of multiple interactions.[21] However, reproducibility of the primary peak rupture force, particularly at 1.0 μm s^{-1}, in the pH and control studies suggests that these forces are attributable to single molecular interactions. Furthermore, the probabilities of specific rupture events for the control studies are consistent with Poisson analysis for single molecular interactions, which suggests that when the probability of observing a rupture event is below 10%, then 95% of the rupture events observed are attributable to single molecular unbinding.[21]

To confirm that the DHFR molecule is in an active form and that forces recorded were specific to the interaction of DHFR and methotrexate, the methotrexate binding sites on the DHFR molecules were blocked through the addition of free methotrexate. This resulted in a decrease in probability of adhesion, and 92% of force measurements lacked any specific binding event. This low percentage adhesion, a peak force of 93 pN and the narrow force distribution (Fig. 4a, *back slash histogram*) suggest that the forces experienced are single molecular. Furthermore, the decrease in the probability of adhesion with a decrease in available binding sites highlights the specificity of the rupture forces experienced in the experimental system.

A plot of force *versus* the logarithm of retract velocity produced a linear regime in which the gradient is comparable to the standard deviations of the force distributions. Furthermore, the standard deviations remain comparable over this linear regime. Dictated by thermal actuation, forces measured for a single interaction are broadened by kinetics and therefore the standard deviation of forces equals the thermal force scale (gradient of the slope). The maintenance of standard deviations over the linear regime and the comparable values for the thermal force scale and the standard deviations are indicative of a single energy barrier in the dissociation pathway. This linear relationship between rupture force and the logarithm of velocity of unbinding observed for the binary complex of DHFR (Fig. 5)

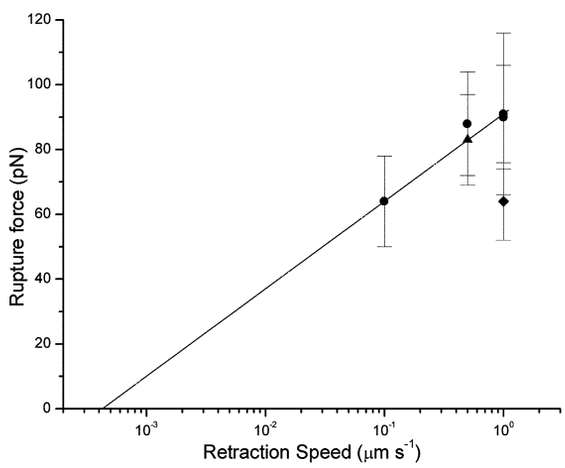

Fig. 5 Representation of rupture forces *versus* logarithm of velocity. *Circle*, binary complex studied at various retract velocities at pH 7.4; *triangle*, ternary complex performed at pH 7.4; *diamond*, binary complex at pH 5.6.

concurs with previous studies performed between other receptor–ligand complexes, such as streptavidin–biotin.[22] Ordinarily, velocity is expressed in the rate of loading (rate × spring constant of the system) to provide an accurate profile of the energy landscape for dissociation. However, in this case the dynamic and mechanical properties of the polymer (agarose bead) and carbon linker employed are unknown, thus the precise rate of loading cannot be identified. If we assume that at the high retract velocities employed the polymeric linker is stretched to its asymptotic regime, where it becomes stiff, then the loading rate should be linear with the retract velocity. Thus, the calculated gradient of the linear regime (force scale) of 12 pN, the comparable standard deviations, and maintenance of the standard deviations over the linear regime (Fig. 5) suggest that the calculated force scale value is a reasonable estimate for the force scale of the transition measured in these studies. A model distribution of force, assuming loading is proportional to retract velocity, was derived using the experimental force scale of 12 pN and the fitted k_{off} of the energy barrier probed (logarithmic intercept at zero force), and applied to the

histograms of rupture forces at given retract velocities. This model distribution is based on the probability a complex will dissociate at a given force, where r_f in our case is velocity, k_{off} is the thermal off-rate of the barrier, and f_β is the force scale.[21]

$$p(f) = \frac{1}{r_f} k_{off} \exp\left(\frac{f}{f_\beta}\right) \exp\left\{-\frac{1}{r_f} f_\beta \cdot k_{off}\left[\exp\left(\frac{f}{f_\beta}\right) - 1\right]\right\} \quad (1)$$

The distance of the probed transition from the bound state can be calculated if f_β of the energy barrier is known.

$$f_\beta = k_\beta T / x_\beta \quad (2)$$

where, k_β is the Boltzmann constant, T is temperature, x_β is the distance between the energy barrier to rupture and a stable minimum.[19] The force scale calculated for a DHFR–methotrexate interaction over the rates studied infers the presence of an energy barrier positioned ≈ 3 Å from the bound state.

However, to reveal the natural lifetime of the interaction requires knowledge of the loading dynamics. Where flexible polymers, such as those employed here, are used to attach the molecular complex to the force transducer, a second timescale is added to that of the interaction. This is a characteristic time to extend the polymer and apply force, and is dependent on the contour and persistence lengths of the attachment. Here these lengths, and hence this time scale, are unknown and therefore the dissociation rate for the probed energy barrier cannot be estimated from the force data.

In order to map the complete dissociation pathway it is necessary to perform studies of applied force over many orders of loading rates.[23] The AFM is unable to achieve such a vast range of measurements, which limits its sensitivity to the energy barriers of unbinding which are situated close to the bound state. To accomplish the wide spectrum of rates necessary to build a profile of the dissociation pathway, the recently developed biomembrane force probe[24] may be employed.

DHFR–MTX–NADPH complex

NMR spectroscopic studies reveal that the conformation of the binary complex (DHFR–MTX) is comparable to that of the ternary complex of *L. casei* (DHFR–MTX–NADPH), suggesting that the NADPH binding site is essentially preformed in the binary complex.[11] AFM force analysis indicates negligible difference in the rupture forces obtained for the binary and ternary complexes. A force of 88 s.d. 16 pN was observed between DHFR and methotrexate (binary complex) (Fig. 4b), and for the ternary complex a rupture force of 83 s.d. 14 pN was obtained (Fig. 6).

The probability of adhesion demonstrated in the experimental system was 20%. The subsequent addition of free methotrexate to the surrounding environment resulted in a decrease in the probability of adhesion to 8%. A comparable peak rupture force, 89 pN, and force distribution were recorded with a control system (Fig. 6, *grey histogram*), emphasising that forces experienced are characteristic of single molecular interactions.

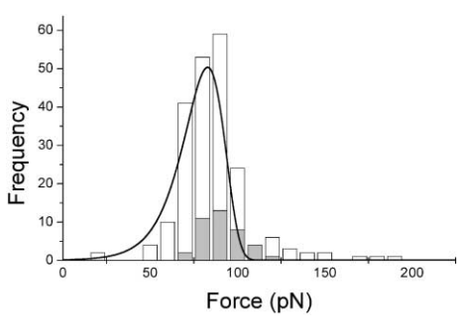

Fig. 6 Frequency distribution histogram of rupture forces of 83 ± 14 pN demonstrated between DHFR–methotrexate–NADPH, performed at a retract velocity of 0.5 μm s^{-1} (*white* histogram). The *grey* histogram represents the control block force measurements. Superimposed upon the force histograms is the model distribution derived from the experimental force scale of 12 pN.

NMR investigations suggest a cooperative relationship exists between methotrexate and NADPH, in which methotrexate facilitates NADPH binding 700 fold.[17a] Since cooperativity of ligand binding is reciprocal then the coenzyme increases inhibitor binding by an equivalent extent.[15,17a] It is speculated that cooperative binding reflects an increased rate of association based on desirably induced conformational changes[25] or through the preparation of the binding site by removal of the water molecules.[26] Matthews *et al.* suggests conformational changes occur where the 'teen loop' (residues 13–22,*lc*) moves substantially on the binding of NADPH, translating the side chain of Leu19,*lc* to a position where van der Waals contact is made with the pyrazine ring of methotrexate.[25] Additional studies have also demonstrated interactions between the two ligands, cofactor and inhibitor. The nicotinamide ring of NADPH has been shown to make contact with the pyrazine portion of the pteridine ring of methotrexate.[27] Baccanari *et al.* showed that NADPH increases the affinity of bacterial DHFR for inhibitors (diaminobenzylpyrimidines), and affinity varied with degree of methoxy substitution of the inhibitor, suggesting that cooperativity is related to hydrophobic and van der Waals interactions between the two ligands.[18] Thus the binding constant of the coenzyme and inhibitor is dependent upon the structure of both ligands.[16–18]

Such a cooperative interaction between methotrexate and NADPH is not evident in the rupture forces for the ternary complex at the dissociation rates studied. The rupture force and force scale (f_β) of methotrexate unbinding in the ternary complex fall within the linear regime for the binary complex (Fig. 5). This suggests that the proposed increase in binding affinity of methotrexate in the presence of the cofactor, as demonstrated by NMR and fluorescence quenching studies, occurs outside the transition probed in this series of studies (Fig. 5).

Protonation of Asp26

The carboxylic acid side chain of the Asp26 residue of the free enzyme has a pK_a of 6.3,[8] and a reduction of the pH below the pK_a results in the protonation of the residue. The decrease in pH resulted in a decrease in the force required for dissociation. At pH 7.4 and a retract velocity of 1.0 μm s^{-1} a force of 90 s.d. 16 pN was observed (Fig. 4a, *grey histogram*). The rupture force decreased to 64 s.d. 12 pN at pH 5.6 (Fig. 7). The addition of free methotrexate resulted in a reduction in the percentage adhesion from 16% to 6%, yielding a peak rupture force and force distribution comparable to the experimental system (Fig. 4a, *forward slash histogram*).

The observed decrease in rupture force with pH suggests that the protonation of the Asp26 residue results in the disruption

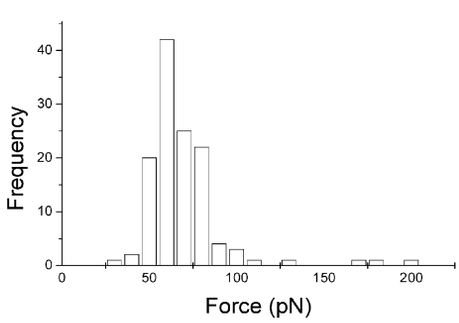

Fig. 7 Frequency distribution histogram of rupture forces of 64 ± 12 pN demonstrated between DHFR–methotrexate, at pH 5.6, 100 mM sodium phosphate. Performed at a retract velocity of 1.0 μm s^{-1}.

of bond formation. If we were to refer to the crystallographic hydrogen bonding maps of the *L. casei* DHFR–methotrexate interaction produced by Bolin *et al.*[3] (Asp26, Thr116 and Wat201 form a highly constrained binding pocket with complementary geometry and charge to the N1 and 2-amino group of the pyrimidine ring of methotrexate), then the observed decrease in force with protonation of the Asp26 residue may be indicative of the disruption in bond formation between either the residue and methotrexate (N1 or 2-amino group) or the residue and the enzyme (Thr116,*lc* or Wat201,*lc*). However it is not possible with this series of studies to precisely identify the specific bonds disrupted by the decrease in pH.

Conclusions

Through the rate studies we have demonstrated the potential of the AFM to investigate regions of the dissociation pathway of drug–enzyme complexes. A linear regime between the logarithm of retract rate and force, for the dissociation of the DHFR–methotrexate complex over the retract rates studied, gave rise to a single energy barrier positioned approximately 3 Å from the bound state. The cooperativity experienced in the association of the ternary complex[15–18,24–26] was not mirrored in the dissociation of the complex for the region studied. In addition, the protonation of the Asp26 residue is known to cause a disruption in bond formation between DHFR and methotrexate,[3] thus the decrease in force observed with a decrease in pH is suggestive of this perturbation.

Experimental

Sample preparation

Utilising a preparation method[28] modified from Vinckier *et al.*, 1995,[29] a concentration of 0.03 mg mL^{-1} *L. casei* DHFR (NIMR, Mill Hill, UK) was covalently immobilised onto polished silicon wafers (Elkis, UK), *via* the ε-amino groups of the lysine residues presented on the surface on the protein. Prior to AFM analysis the DHFR samples were rinsed thoroughly in high-purity deionised water (purified using an ELGA water system, resistivity 15 MΩ cm) to remove any non-covalently bound protein.

Probe functionalisation

Silicon nitride (Si_3N_4) cantilever probes (Digital Instruments, Santa Barbara, CA) were functionalised by the attachment of a methotrexate modified agarose bead. Methotrexate was covalently bound to the agarose bead *via* an 8-atom carbon linker (Sigma, Poole, UK), which reduces steric hindrance and promotes single molecular interactions. The drug-modified bead was attached to the apex of the cantilever using an Araldite-Rapid™ epoxy adhesive (Bostik Ltd, Leicester, UK). Positioning of the bead was achieved under an optical microscope using a micromanipulator (Research Instruments Ltd, Cornwall, UK).

AFM analysis

AFM force measurements were obtained in 100 mM sodium phosphate buffer, pH 7.4, unless otherwise stated. Force data were obtained as plots of cantilever deflection signal (nA) *versus* distance of z-piezo movement (nm). Plots were converted to force (nN) *versus* probe–sample distance (nm).

The cantilever spring constants were calibrated with the methotrexate-modified agarose bead attached, using the cantilever thermal noise fluctuation method.[30] The calibration of spring constants following the attachment of the bead encompasses the potential effects the presence of the bead and glue may have on the compliance of the cantilever. The diameters of the hydrated MTX-modified agarose beads were 40 ± 6 μm and contribute marginally to the hydrodynamic force present in the system. The hydrodynamic drag applied to a 40 μm bead over the velocities studied was estimated using Stokes' Law, where η is the viscosity of the suspension medium (water is 0.001002 N m^{-2} s at a temperature of 293 K),[31] r is the sphere radius (m) and v is the velocity (m s^{-1}).

$$F = 6\pi\eta r v \quad (3)$$

At 1.0 μm s^{-1} a hydrodynamic force of 0.38 pN is exerted on a 40 μm bead, at 0.5 μm s^{-1} a force of 0.19 pN is exerted, and at 0.1 μm s^{-1} a force of 0.038 pN. Such forces are well within the instrumental noise (~10 pN), thus will have a negligible effect upon our measurements. It should be noted that the effect of cantilever hydrodynamics and bead inertia upon rupture force values is at present poorly understood and is currently a subject of research.

Rupture forces indicative of specific interactions were plotted as histograms. The histogram peak values were plotted as a function of logarithm of the retract velocity. f_β was calculated, and using eqn. (1) a model distribution was derived and overlaid onto the histograms.

Experimental retraction rates. Force measurements were obtained between a methotrexate functionalised AFM probe and a DHFR sample surface (Fig. 2), at retract rates of 1.0 and 0.1 μm s^{-1}. Measurements were performed using an AFM instrument built and developed in our laboratory.[32]

DHFR–MTX–NADPH complex. Force measurements were obtained between methotrexate and DHFR, in the presence and absence of 1.2 μg mL^{-1} NADPH (Sigma, Poole). Measurements were recorded at a retraction rate of 0.5 μm s^{-1}, using a commercial AFM instrument, Molecular Force Probe (Asylum Research, California).

Protonation of Asp26. Force measurements were recorded between methotrexate and DHFR, at pH 7.4 and 5.6, 100 mM sodium phosphate buffer. Measurements were acquired at a retraction rate of 1.0 μm s^{-1}, using an AFM instrument built and developed in our laboratory.

For each investigation a control procedure was performed to ensure that the adhesive interactions observed were specific in nature, and that the DHFR was present in an active form. The methotrexate binding sites on the DHFR molecules were blocked through the addition of free methotrexate into the experimental systems (Sigma, Poole). DHFR samples were incubated in 0.64 μg mL^{-1} methotrexate (100 mM sodium phosphate buffer, pH 8.0) for a period of 1 h at room temperature. Measurements were then re-recorded.

All force measurements were repeatable at the same point on the sample surface, indicating that the functionalised methotrexate bead probe remained intact during measurements and that the DHFR molecules were not being pulled off the silicon wafer during the experimental studies. The same functionalised probe was used to acquire all force data throughout both the experimental and control systems. It was necessary to utilise the same probe in order to prevent the introduction of unnecessary errors due to variations in spring constant of the cantilever probe and methotrexate bead size.

Acknowledgements

The authors would like to thank J. Feeney for the generous supply of *L. casei* DHFR, and for valuable discussions. SRS thanks Ortho-Clinical Diagnostics and the University of Nottingham for funding her studentship. SA would like to thank Pfizer Global Research and Development for funding her lectureship. PMW is an EPSRC Advanced Research Fellow.

References

1 R. L. Blakely, *The biochemistry of folic acid related pteridines*, North-Holland Publishing Co., Amsterdam, 1969.
2 C. Bystroff and J. Kraut, *Biochemistry*, 1991, **30**, 2227–2239.
3 J. T. Bolin, D. J. Filman, D. A. Matthews, R. C. Hamlin and J. Kraut, *J. Biol. Chem.*, 1982, **257**, 13650–13662.
4 C. Bystroff, S. J. Oately and J. Kraut, *Biochemistry*, 1990, **29**, 3263–3277.
5 M. R. Sawaya and J. Kraut, *Biochemistry*, 1997, **36**, 586–603.
6 J. Feeney, *Angew. Chem., Int. Ed.*, 2000, **39**, 290–312.
7 B. Birdsall, A. M. Gronenborn, E. I. Hyde, G. M. Clore, G. C. K. Roberts, J. Feeney and A. S. V. Burgen, *Biochemistry*, 1982, **21**, 5831–5838.
8 S. R. Stone and J. F. Morrison, *Biochemistry*, 1984, **23**, 2753–2758.
9 L. F. Kuyper, B. Roth, D. P. Baccanari, R. Ferone, C. R. Beddell, J. N. Champness, D. K. Stammers, J. G. Dann, F. E. A. Norrington, D. J. Baker and P. J. Goodford, *J. Med. Chem.*, 1982, **25**, 1120–1122.
10 (*a*) D. A. Matthews, J. T. Bolin, J. M. Burridge, D. J. Filman, K. W. Volz, B. T. Kaufman, C. R. Beddell, J. N. Champness, D. K. Stammers and J. Kraut, *J. Biol. Chem.*, 1985, **260**, 381–391; (*b*) D. A. Matthews, J. T. Bolin, J. M. Burridge, D. J. Filman, K. W. Volz and J. Kraut, *J. Biol. Chem.*, 1985, **260**, 392–399.
11 A. R. Gargaro, A. Soteriou, T. A. Frenkiel, C. J. Bauer, B. Birdsall, V. L. Polshakov, I. L. Barsukov, G. C. K. Roberts and J. Feeney, *J. Mol. Biol.*, 1998, **277**, 119–134.
12 J. P. Perkins and J. R. Bertino, *Biochemistry*, 1966, **5**, 1005–1012.
13 F. Otting and F. M. Heunnekins, *Arch. Biochem. Biophys.*, 1972, **152**, 429–431.
14 G. C. K. Roberts, J. Feeney, A. S. V. Burgen, V. Yuferov, J. G. Dann and R. A. Bjur, *Biochemistry*, 1974, **13**, 5351–5357.
15 J. W. Williams, J. F. Morrison and R. G. Duggleby, *Biochemistry*, 1979, **18**, 2567–2573.
16 B. Birdsall, A. S. V. Burgen, J. Rodrigues de Miranda and G. C. K. Roberts, *Biochemistry*, 1978, **17**, 2102–2110.
17 (*a*) B. Birdsall, A. S. V. Burgen and G. C. K. Roberts, *Biochemistry*, 1980, **19**, 3723–3731; (*b*) B. Birdsall, A. S. V. Burgen and G. C. K. Roberts, *Biochemistry*, 1980, **19**, 3732–3737.
18 D. P. Baccanari, S. Daluge and R. W. King, *Biochemistry*, 1982, **21**, 5068–5075.
19 E. Evans, *Faraday Discuss.*, 1998, **111**, 1–16.
20 O. H. Willemsem, M. M. Snel, L. Kuipers, C. G. Figdor, J. Greve and B. G. De Grooth, *Biophys. J.*, 1999, **76**, 716–724.
21 P. M. Williams and E. Evans, unpublished work.
22 E. Evans and K. Ritchie, *Biophys. J.*, 1997, **72**, 1541–1555.
23 R. Merkel, P. Nassoy, A. Leung, K. Ritchie and E. Evans, *Nature*, 1999, **397**, 50–53.
24 E. Evans, K. Ritchie and R. Merkel, *Biophys. J.*, 1995, **68**, 2580–2587.
25 D. A. Matthews, R. A. Alden, J. T. Bolin, D. J. Filman, S. Freer, R. Hamlin, W. G. J. Hol, R. L. Kisliuk, E. J. Pastore, T. Plante, N. Xuong and J. Kraut, *J. Biol. Chem.*, 1978, **253**, 6946–6954.
26 J. Feeney, personal communication.
27 D. A. Matthews, R. A. Alden, S. T. Freer, N. Xuong and J. Kraut, *J. Biol. Chem.*, 1979, **254**, 4144–4151.
28 S. Allen, X. Chen, J. Davies, M. C. Davies, A. C. Dawkes, J. C. Edwards, C. J. Roberts, J. Sefton, S. J. B. Tendler and P. M. Williams, *Biochemistry*, 1997, **36**, 7457–7463.
29 A. Vinckier, I. Heyvaert, A. D'Hoore, T. McKittrick, C. Van Haesendonck, Y. Engelborghs and L. Hellemans, *Ultramicroscopy*, 1995, **57**, 337–343.
30 J. L. Hutter and J. Bechhoefer, *Rev. Sci. Instrum.*, 1993, **64**, 1868–1873.
31 The viscosity of water at 20 °C, 0.001002 N m^{-2} s, was taken from the National Standards Commission, www.nsc.gov.au.
32 M. Lomas, PhD Thesis, The University of Nottingham, United Kingdom, 1999.